Valentina Gianotti; Giada Favaro; Luca Bonandini; Luca Palin; Gianluca Croce; Enrico Boccaleri; Emma Artuso; Wouter Van Beek; Claudia Barolo; Marco Milanesio. Rationalization of dye uptake on titania slides for dye-sensitized solar cells by a combined chemometric and structural approach. CHEMSUSCHEM. 7 (11) pp: 3039-3052.
DOI: 10.1002/cssc.201402194

Rationalization of dye uptake on TiO_2 slides for Dye-sensitized Solar Cells by a combined chemometric and structural approach

Valentina Gianotti,[a] Giada Favaro,[a] Luca Bonandini,[b,c] Luca Palin,[a] Gianluca Croce,[a] Enrico Boccaleri,[a] Emma Artuso,[b] Wouter van Beek,[d] Claudia Barolo*[b] and Marco Milanesio*[a]

[a] *Dipartimento di Scienze e Innovazione Tecnologica, Università del Piemonte Orientale "A. Avogadro", Viale T. Michel 11, I-15121 Alessandria, Italy Fax: + 39 0131 360250; Tel: + 39 0131 360226; E-mail: marco.milanesio@unipmn.it*

[b] *Dipartimento di Chimica, NIS Interdepartmental Centre, Università di Torino, Via Pietro Giuria 7, I-10125, Torino, Italy Fax: +39 011 6707591; Tel: +39 011 6707596; E-mail: claudia.barolo@unito.it*

[c] *DYEPOWER, Viale Castro Pretorio 122, 00185 Roma-Italy*

[d] *Swiss-Norwegian Beamlines at ESRF, BP 220, Grenoble, 38043, France*

A model photosensitizer (D5) for application in Dye-sensitized Solar Cells has been studied by a combination of X-ray diffraction, theoretical calculations and spectroscopic/chemometric methods. The conformational stability and flexibility of D5 and molecular interactions between adjacent molecules was characterized to obtain the driving forces governing D5 uptake and grafting process, and to infer the most likely arrangement of the molecules on the surface of titanium oxide. A spectroscopic/chemometric approach was then used, yielding information about the correlations between three variables governing the uptake itself: D5 concentration, dispersant (chenodeoxycholic acid, CDCA) concentration and contact time. The obtained regression model shows that large uptakes can be obtained at high D5 concentrations, when CDCA is present and contact time is high, or, in absence of CDCA, only if contact time is smaller, suggesting how to optimize dye uptake and photovoltaic device preparation.

1. Introduction

Photovoltaic (PV) cells based on organic semiconductors and/or organic light harvesters are potentially extremely inexpensive, but their efficiency and stability are still limited when compared to inorganic crystalline solar cells. Among them, Dye-sensitized Solar Cells (DSC) represent a promising and emerging technology.[1] These cells mimic the energy conversion mechanism of photosynthesis, since light is absorbed by an antenna compound (chlorophyll in photosynthesis, a dye in DSC), then an excited electron is produced and captured by a complex system (photo systems I and II in photosynthesis and nanostructured titanium oxide, tin oxide and an inorganic electrolyte in DSC), that exploits the energy to obtain valuable products (i.e. chemical energy in the form of sugar in photosynthesis and electric current in DSC).

The chemical properties of the cell components must be designed and tuned in a careful way to optimize the yield of PV cells. Presently the main issues that still limit their technological applications[2] are: (i) obtaining reasonable (10% for opaque, 5-6% for transparent) conversion efficiency of the DSC modules,[3] (ii) maintaining these yields during the years (~20) needed for a cell working in real conditions, (iii) obtaining reproducible results (± 3-5% differences between modules). To fulfil these objectives, a detailed molecular-level knowledge of the DSC components is of paramount importance.

Even if a great deal of research has been carried out to design more efficient photosensitizers,[4] only recently some efforts have been made in understanding,[5,6] modelling[7-10] and controlling[11] of the interactions that play a major role in the dye uptake. Moreover, the dye loading amount can be tuned by changing the bath solvent,[5] which has an important effect on the cell efficiency. Literature data clearly highlighted also the importance of *CDCA* as co-adsorbent to control dye aggregation and electron injection[12] and to improve performances.[13] However a rationalization of the effect of chemical parameters affecting dye uptake, in relation with chemical forces governing molecular interactions is still lacking. The ***D5*** dye, proposed by Hagberg et al.,[14] can be referred as case study for the rationalization of uptake conditions in metal-free dyes. In fact this simple molecule[7,15] can be considered as a model for the widespread class of Donor-π-Acceptor (D-π-A) dyes. This class retains to date the efficiency record for metal-free dyes.[16] In the last decade, various organic functional groups have been combined to generate D-π-A structures. One among the most commonly employed schemes is: the aryl-amine group as electron donor, the thiophene unit as π linker, and the cyanoacrylic-acid moiety as the electron acceptor/anchoring group (all of them already present in the ***D5*** molecule).

Structural and crystallographic studies on organic compounds and molecular complexes allow assessing the possible intra- and inter-molecular interactions, which are of paramount importance for the functionality of the materials in working conditions.[17-19] Very few structural studies can be found in the DSC field because of the complications of dye crystallography, mainly due to the difficulty of obtaining suitable single crystals. Ru-based dye compounds[20] are less difficult to be crystallized and represent the majority among the X-ray crystal structures related to DSC, while only few crystal structures of compounds related to D-π-A sensitizers are available on the CCDC.[21] Relevant structures in the database are: i) a molecule containing the diphenylamino-phenyl and the carboxylic moieties, i.e. a ***D5*** without the vinyl-thiophene linker;[22] and ii) two molecules containing the diphenylamino-phenyl moiety and a thiophene linker.[23] The electronic and molecular surface structure of the functional dye-sensitized interface has also been studied in detail for the ***D5*** molecule by a combination of core level spectroscopy, valence level spectroscopy, x-ray absorption spectroscopy, and resonant photoemission spectroscopy.[24]

In this paper we intend to shed some light on the dye uptake process combining a Design of Experiment (DoE) assisted UV-Vis spectroscopy with a structural investigation. Our aim is to understand the mechanism of dye dispersion and bonding onto the TiO_2 surface, with the long term goal of understanding their influence on the cell macroscopic behaviour. In the present study, the dye related crystallography problems have been overcame by exploiting advanced powder diffraction methods, using different high resolution detectors on a high flux synchrotron radiation X-ray source. We report on the crystal and molecular structure of the polyene-diphenylaniline dye ***D5***, and two related compounds (**4** and **6** in Scheme 1**)** by powder and single crystal X-ray diffraction respectively. The analysis of their packing features allowed understanding the molecular forces governing their intra- and inter-molecular interactions. However crystallographic studies cannot give direct information on the behavior of ***D5*** on titania. In order to shed light on the correlations between the main parameters governing the dye uptake, a chemometric-driven UV-Vis spectroscopic study was designed and performed. UV-Vis spectroscopy was used recently by Dell'Orto et al. to assess the kinetics of absorption of the N719 dye onto titania.[11] We choose to exploit a quantitative chemometric approach because it allows maximizing the information content with the least number of experiments.[25-27] Up to now, the optimization of the experimental conditions of dye uptake was carried out mainly by trial and error or at best by "*One Variable At a Time*" (OVAT) methods. Only very recently the chemometric approach was proposed in the DSC field by some of us.[28] The present work aims at investigating both the molecular structure and the dye uptake in a synergic way and represents the first part of a larger project we are carrying out with the purpose of understanding, at the molecular level, the mechanisms involved in DSC functioning, with the final aim of improving their yields and stability by optimizing the preparation methods of the cell itself.

2. Results and Discussion

2.1 *D5* synthesis

Syntheses of compounds **4** and ***D5*** were performed with a slight modification compared to the literature procedures,[14,29] starting from commercial 4-(*N*,*N*-diphenylamino)benzaldehyde **1** (Scheme 1). The first step of our synthetic pathway is a simple Wittig reaction[30] to obtain alkene **2** which was used as a substrate for a subsequent Pd-catalyzed decarbonylative Heck reaction[31] to give intermediate **3**. Subsequently, lithiation of **3** with *n*-butyllithium followed by the addition of DMF yielded the corresponding aldehyde **4**. The electron-withdrawing group is inserted in the structure by a Knoevenagel reaction between aldehyde **4** and cyano acetic acid in the presence of piperidine.

D5 dye was then converted into its corresponding methyl ester (**6**) to verify the configuration of the 2-cyano-3-(thiophen-2-yl) acrylic moiety. Compound **6** was also obtained, in the same configuration, through the classical Knoevenagel reaction directly from **4**.

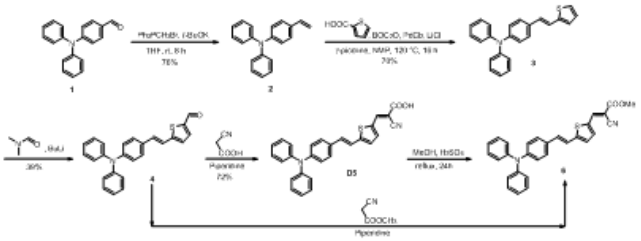

Scheme 1: Synthesis of ***D5*** dye.

2.2 Computational study of *D5* conformational flexibility and freedom

The chemical formula of ***D5*** (Figure 1) suggests that this molecule should be rather rigid and planar, because of the conjugation between aromatic moieties (thiophene and benzene rings) trough a C=C double bond. In addition the cyano-acetic group is planar and connected to thiophene by a double bond. The only non rigid part is the three-phenyl-amino moiety, which is non planar with the terminal phenyl groups free to rotate and adopt different conformations. The crystal structures of compounds **4** and **6** from single crystal data gave a clear picture of the stereochemistry around the C=C double bond isomerisation, and confirmed the expected E isomer (see section 2.3). Besides, NMR and chromatography experiments (see ESI, Section 1) confirmed that also in solution only one isomer is present. Conversely, a rather rich conformational variability can arise because of the rotation around the single bonds, as discussed below. A reliable indication about the stable conformation of ***D5*** in the solid state could in principle be gained from single crystal diffraction data, but the same indication about the dye in solution or when bonded to the titania surface, can only be obtained, lacking direct information, by a combination of experimental X-ray data (section 3.4) and computational analysis by first principle calculations (this section). Having failed all our attempts at growing single crystals of ***D5*** because of the well known difficulty of crystallizing bulky carboxylic acids, in analogy to what observed for fatty acids,[32] high resolution X-ray powder diffraction (XRPD) was thus used. The limited resolution of XRPD on organic molecules rendered the discrimination between the isomers rather difficult and therefore an accurate conformational analysis was needed.

2.2.1 First principle calculations on stable minima

In the literature,[9] only one isomer of ***D5*** (named ***D5*-2a** in Table 1) is generally accepted and used.[33] Lacking a single crystal structure of ***D5***, and being almost impossible to directly and precisely investigate the structure of ***D5*** onto titania and in

solution during the grafting process, accurate first principle theoretical calculations, combined with an experimental structural study of ***D5*** and parent compounds, have been carried out and reported in detail in a separate paper, together with all strategies and tricks used for structure solution.[34]

In this paper the possible conformational changes were investigated considering the three degrees of freedom (named ϕ_1, ϕ_2 and ϕ_3 and identified in Figure 1), which can assume either the *s-cis* or the *s-trans* conformations, being E/Z isomerisation already established. The conformational changes around ϕ_4, ϕ_5 and ϕ_6 are less important because of the symmetry of the phenyl groups. However, for an exhaustive search they were also considered, but only the more stable conformations of ***D5*** and related compounds are reported (see Table SI-2 for detailed geometric features).

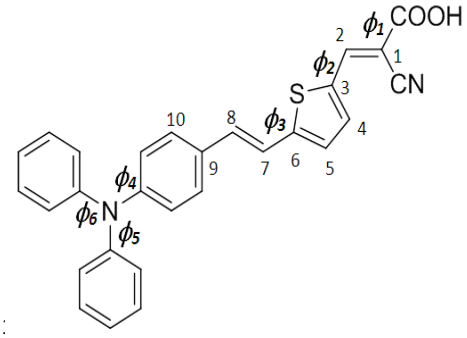

Figure 1: Degrees of freedom of *D5* molecule: ϕ_1, ϕ_2 and ϕ_3 refer to O=C-C1=C2, C1=C2-C3=C4 and C5=C6-C7=C8 torsion angles respectively.

Among the possible theoretical conformers, four of them (namely ***D5*-1a**, ***D5*-1b**, ***D5*-2a** and ***D5*-2b**) possess stable energy minima below 1.5 Kcal/mol. According to Boltzmann distribution, they are, most probably, the dominant ones for ***D5*** in solution and on the titania surface (i.e. in the relevant cases).

Table 1. Geometric features using B3LYP functional of the more stable conformers (within 1.5 Kcal mole^{-1}) conformers after geometric optimizations.

	Φ_1 (°)	Φ_2 (°)	Φ_3 (°)	[a]	[b]	[c]
***D5*-1a**	0.1	180	180	0.00	0.00	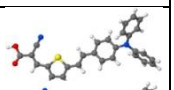
***D5*-1b**	0.0	180.	-1.1	0.95	0.73	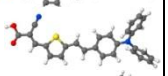
***D5*-2a**	0.0	0.1	180	0.38	0.34	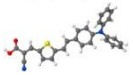
***D5*-2b**	0.0	0.1	-1.8	1.29	0.98	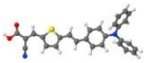
4	---- ----	-178 -179	-177 4.7			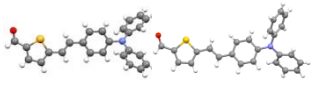
D5	-9.3 0.6	-173 -168	-169 -175			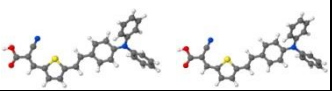
6	-0.9	179	166			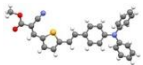
	[a] 6-31G(d,p); [b] 6-311+G(2d,2p); [c] Molecular structure.					

The geometries of the four isomers, after geometric optimization by first principle calculations at the B3LYP/6-31G(d,p) and B3LYP/6-311+G(2d,2p) levels of theory, are depicted in Table 1. 6-31G(d,p) basis set was used to obtain a first fast geometry optimization and screening of possible stable conformations, while 6-311+G(2d,2p) basis set was mandatory to get a careful description of molecular geometries of the conformers and of their relative stabilities.Conformer ***D5*-1a** is the most stable and also the most present in X-ray crystal structures (see section below) and thus can be considered the prevalent one at the

equilibrium, The most commonly reported one (***D5*-2a**)[14,16] and the other two conformers are less stable by less than 0.5 kcal mol^{-1} and can be present at lower concentrations in solution, according to Boltzmann distribution, and at not equilibrium conditions. It must be noted that, in the case when ***D5*** is at first approaching and then linked to the titania surface, the carboxyl group is deprotonated and the conformational degree of freedom around ϕ_1 becomes irrelevant because the COO^- moiety is symmetric for a 180° rotation. Moreover in the deprotonated ***D5*** the energy differences are even smaller (Table 2).

Table 2. Relative stabilities (kcal $mole^{-1}$) after geometric optimization of the more stable conformers for the four models employed in the theoretical calculations

	4		**Depr_*D5*$^-$**		**6**	
	[a]	[b]	[c]	[d]	[e]	[f]
***D5*-1a**	0.00	0.00	0.00	0.00	0.00	0.00
***D5*-1b**	0.98	0.75	1.24	1.11	0.97	0.77
***D5*-2a**	1.55	1.41	-0.59	-0.51	0.36	0.31
***D5*-2b**	2.46	2.05	0.79	0.66	1.28	0.99
	[a] 6-31G(d,p), [b] 6-311+G(2d,2p); [c] 6-31G(d,p), [d] 6-311+G(2d,2p); [e] 6-31G(d,p), [f] 6-311+G(2d,2p).					

The theoretical calculations suggest therefore that conformers ***D5*-1a**, ***D5*-1b**, ***D5*-2a** and ***D5*-2b** are the most probable ones. In fact, three out of these four conformations were experimentally observed in the X-ray crystal structures (see discussion below in the dedicated section), where crystal packing forces play a relevant role in the selection of less stable conformers. The compromise between the intrinsic thermodynamic stability of the isolated conformers and the effect of inter-molecular interactions in the solid-state is well known as observed when comparing theoretical calculations with X-ray structures.[35] Of course, these conclusions do not take into account the energy barriers for rotation around the C-C bonds, investigated in the next paragraph

2.2.2 Energy barriers between energy minima as a function of torsion angles

The rotation barriers between the four conformers were explored by Relaxed Potential Energy Scans (R-PES) around the 2 S-C-C=C torsion angles (ϕ_2 and ϕ_3). To explore at best this energy surface, with an acceptable computing time, at first two, one-dimensional, R-PES scans were carried out at the same DFT level (B3LYP/6-31G(d,p) and the data are reported in Figure 2a. Then a two-dimensional R-PES at the less demanding HF/3-21G level of calculation was carried out exploring, at the same time, the two torsions thus producing the 3D plot reported in Figure 2b. The basis sets used for geometry optimizations would be too much time consuming and unaffordable for such an extended PES. However HF-3-21G still gave acceptable geometries and energy differences when comparing the energy minima to the results of the more extended basis sets.

(a)

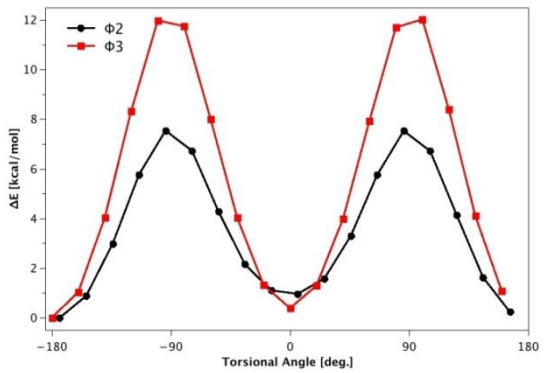

(b)

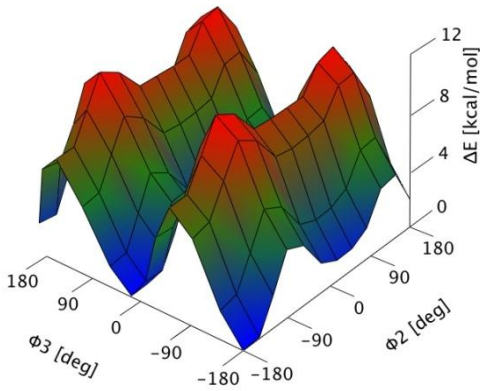

Figure 2: (a) Energy profiles for rotation around ϕ_2 (black curve) and ϕ_3 (red curve) torsion angles from B3LYP/6-31G(d,p) calculations, all geometries were fully optimized except for the imposed values of the ϕ_2 and ϕ_3 torsion angles; (b) 3D plot of energies obtained from the 2D R-PES

The observed minima confirmed at first that the *s-cis* conformation of ***D5*-1a** is favoured and the other three conformers (***D5*-1b**, ***D5*-2a**, ***D5*-2b**) are the unique stable minima, in agreement with the first principle DFT calculations. The R-PES indicated that rotation around ϕ_2 is easier than around ϕ_3. Moreover there are no other minima and there are no sterically forbidden regions hindering the rotation. The heights of the barrier (about 4 and 10 kcal/mole around ϕ_2 and ϕ_3) suggest that during ***D5*** manipulation, for both the DoE-assisted uptake experiment here used and, in general, for DSC cell preparation, rotation around this single bond is possible, as also indicated by the fact that compounds **4**, ***D5*** and **6** show different conformations in their crystal structures. This conformational flexibility is probably important in driving the ***D5*** uptake on titanium oxide as well as the final arrangement of ***D5*** molecules on its surface. The absolute minimum of the calculations (conformer **1**) shows *s-trans* conformation for both ϕ_2 and ϕ_3 torsion angles, while the conformation usually considered in the literature (conformer **2**) shows *s-cis* and *s-trans* conformations for ϕ_2 and ϕ_3 respectively. Both conformations are very close in energy and therefore accessible at RT conditions. The larger stability of *s-cis* conformation suggested by first principle calculations was confirmed by searching distribution of *s-cis* and *s-trans* conformation in the structures containing the vinil-thiophenic moiety in CCDC database.[21] This search (Figure SI-4) confirmed a large prevalence of *s-trans* conformation.

2.3 Crystal structures* of *D5*, of its precursor (4) and of its methyl ester (6)

The conformational flexibility suggested by first principle calculations had to be confirmed by experimental crystallographic data. From compounds **4** and **6**, despite many different attempts, it was not possible to grow a single crystal for ***D5*** and, as explained before, its structure had therefore to be investigated by high resolution synchrotron radiation X-ray powder diffraction. The XRPD study was carried out at ambient conditions, since an experiment at 100K (where better data could be in principle collected) a new phase appeared with formation of a mixture impossible to index. For consistency also compound **4** and **6** were measured at RT. Because of the well known limitations in the accuracy of the structures solved by powder diffraction data, identifying the correct conformations around the ϕ_1, ϕ_2, and ϕ_3 torsion angles without *a priori* information is a rather difficult or even impossible task. In fact the conformations, described in section 3.2 and depicted in Figure 1, have very small electron density differences. Even the high quality of the data recorded with the 1D analyzer detector (BM1B) and the 2D MAR CCD (BM1A) at SNBL did not result sufficient for a successful structure solution, as detailed elsewhere.[34] To overcome the problem, on one hand, high resolution powder diffraction data of excellent spatial and reciprocal space resolution were collected exploiting a Pilatus 2M detector[42] and, on the other hand, data from theoretical calculations and a priori information from the single crystal structures of compounds **4** and **6** were exploited. The crystallization of these two parent compounds resulted much easier and their single crystal structures could give direct and accurate indications about the more stable conformation in the solid state. It is worth noting that both structures **4** and **6** showed that the most stable conformations coincide with the more stable from first principle calculations. This information helped the interpretation of powder diffraction data from ***D5***. At first the single crystal structure of the compound **4**, (sect 2.3.1) was solved to determine the torsion angle ϕ_3 and the common geometric features of these compounds, i.e the planarity of the thiophene group and the geometry of the diphenylamino chromophore. Then, compound **6** (a crystalline derivative of ***D5***) (sect 2.3.1) was prepared to obtain experimental data from XRD single crystal data to shed light on the conformational features of the 2-cyanoacrylic moiety, i.e. on the conformation around the ϕ1 and ϕ2 torsion angles. In the following sections the relevant features of the three structures are discussed, while all crystal data are reported in the ESI file.

*2.3.1 Single crystal structures of compound **4** and compound **6***

Compound **4** crystallizes in the *P-1* space group and the asymmetric unit contains two molecules arranged in a parallel fashion along their elongation axis, but rotated by about 90° one with respect to the other to form *T*-like interactions between the aromatic conjugated moieties, as can be seen in Figure 3. The two molecules show two different conformations (*s-cis*, *s-trans*) for the ϕ_3 torsion angle (see Table 1), confirming the possibility of more than one stable conformation suggested by theoretical calculations. Conversely ϕ_2 shows an *s-trans* conformation in both molecules. A short S••••O intra-molecular contact (d_{mean}= 3.04(8) Å) is observed.

Concerning the triphenylamine group, the nitrogen atom is very close to an sp^2 hybridation, since the three C-N-C angles are between 118 and 122° and the torsion angle defining the piramidality of N (i.e. the one obtained by the N itself and the three C atoms bonded to the N), is very close to the 0° value, as expected for a perfect sp^2 hybridation. The two terminal phenyl groups are not co-planar in order to minimize their reciprocal steric hindrance. The remaining part of the molecule is planar with deviations smaller than 4° in all torsion angles, also for ϕ_1 and ϕ_2. Finally hydrophobic inter- and intra-molecular interactions between the phenyl groups of the dibenzylaminic moieties are present.

(a)

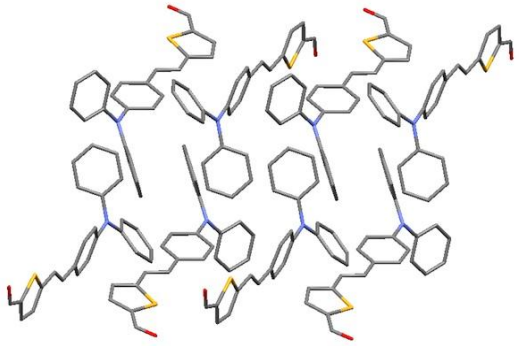

(b)

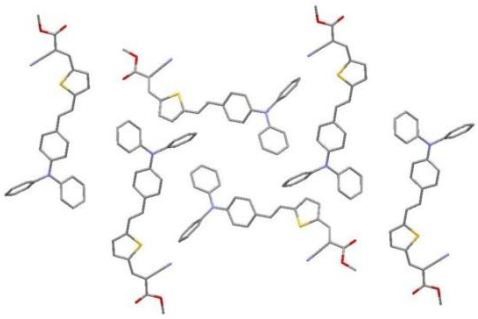

Figure 3: Crystal packing of compound **4** (a) and **6** (b) highlighting the hydrophobic clustering of phenyl groups in both cases.

Compound **6** crystallized in the $P2_1/c$ space group with one molecule in the asymmetric unit. The triphenylamine and the thiophene moieties reveal geometries similar to those of compound **4** and also the cyano-acetic group is coplanar with the rest of the molecule. The most relevant information is given by the conformational arrangement around the ϕ_2 and ϕ_3 torsion angles, both close to 180° with *s-trans* conformation within 6° (see Table 1), as in the absolute minimum of first principle calculations. A short S••••N intra-molecular contact (d=3.26(7) Å) is observed. The crystal packing of compound **6** is exclusively driven by short contact interactions (less than the sum of van der Waals radii), because no H-bond is possible. Hydrophobic interactions between phenyl moieties are observed, similarly to compound **4**. Furthermore the molecular packing also reveals that the short contact network is formed by the intermolecular interaction between the triphenylamine and cyanoacetic groups of adjacent molecules.

2.3.2 ***D5*** *structure from X-ray powder diffraction data*

The unit cell of ***D5*** can contain four molecules and, given the *P-1* symmetry with only the inversion centre as symmetry element, two molecules must be present in the asymmetric unit. To solve the structure without biasing the search and exploring at best the structure solution hyper-surface, all four stable isomers ***D5*-1a**, ***D5*-1b**, ***D5*-2a**, ***D5*-2b**, were used as starting guess for the real space structure solution of ***D5***, also combining two molecules with different conformations, as observed for compound **4**. When the simulated annealing searches are sufficiently extended, in terms of temperature and time, the results converged to a solution with ϕ_2 close to 0°, while acceptable solutions were obtained with ϕ_3 close to both 0° and 180°. In other words, two possible correct structure solutions are suggested by simulated annealing. The first has two molecules with conformation ***D5*-1a** and small differences in the planarity of the vinyl-thiophene moiety and in the arrangement of the three phenylamino groups, the latter has two different conformations, ***D5*-1a** and ***D5*-1b**, as observed in compound **4**. Conformations ***D5*-2a** and ***D5*-2b** do not appear in any possible stable solutions among the highly ranked R values. The best fitting of the XRPD data (see figure SI-3 in ESI file) was obtained for the first arrangement with two molecules ***D5*-1a** (the absolute minimum of first principle calculations) in the asymmetric unit (see Table 1).

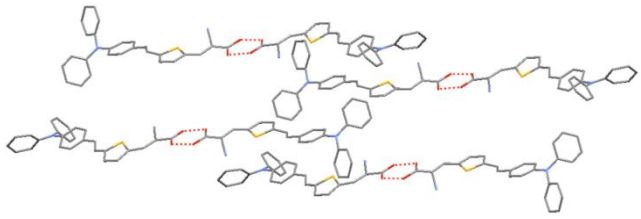

Figure 4: Crystal packing of *D5*, showing H-bonds and hydrophobic interactions between aromatic groups.

The packing driving forces are head-tail hydrogen-bonds between the COOH moieties of adjacent ***D5*** molecules (Figure 4). Hydrophobic clustering of phenyl groups are observed as in compounds **4** and **6**. It can be concluded that the phenyl-phenyl interactions are the common feature of all 3 solved crystal structures and must be very important also when ***D5*** is bound to titania nanoparticles. Apart from these common features, it is surprising that the crystal packing of ***D5*** and its precursor are different. While parallel π-π stacking interactions are observed in ***D5***, in compound **4** the molecules are pillared in a perpendicular way with *T*-like interactions (see Table SI-4 in ESI). Compound **6** shows a completely different packing without stacking of planar aromatic moieties, but the phenyl-phenyl are still observed. The torsion angles ϕ_2 and ϕ_3 are almost planar (see Table 1) but with deviations, within 10°, larger than those suggested by theoretical calculations (where deviations from 0 and 180° are within 2°, see table SI-4 for a detailed comparison). Such freedom is indeed confirmed by calculated PES, where a

rather flat energy trend is observed between -20 and +20° and -160 and +160° in Figure 2a) and by literature experimental data (see figure SI-4 in ESI file). The variety and richness of molecular interactions and deviation from planarity highlighted by crystallographic and computational studies, probably occurring also in solution and after adsorption on TiO_2 surface, uptake suggest that dye uptake is a complex phenomenon requiring a quantitative study for an optimization on both materials use and cell performances.

2.4 Chemometric study of *D5* uptake

A *Full Factorial Design* (FFD)[‡] was used taking into account all the parameters involved in the dye uptake in order to maximize the information with the minimum number of experiments to be performed. A *Design of Experiment* (DoE[‡]) approach allows, by carrying only 22 experiments, to evaluate in triplicate the effect of three variables on two series of samples (powder and TiO_2 slides). Instead, with a standard 3D experimental grid, 162 experiments (3^3x3x2) would be necessary.

Preliminary experiments with *P25* powder were carried out to estimate the correct range of ***D5*** concentrations for the uptake study. Then a first FFD was carried out using different amounts of *P25* powder put in contact with ***D5*** solutions at different concentrations with and without the presence of a dispersant molecule (chenodeoxycholic acid, *CDCA*), in order to evaluate the effects of these parameters in a model system. Finally a FFD experiment applied to a more complex and realistic model on standard TiO_2 slides was carried out, to explore the mutual influence on the ***D5*** uptake in real systems of the three parameters: ***D5*** concentration, *CDCA* concentration and soaking time (*t*).

The simplest, fastest and non destructive method for dye uptake evaluation is Uv-Vis spectroscopy, that can indirectly, but precisely measure the amount of dye extracted from the solution by both titania powders and TiO_2 slides.[36-37] The direct evaluation of the amount of grafted dye can be done only by disruptive and more time consuming methods such as Uv-Vis spectroscopy after dye desorption (with the implicit risk of partially degrading the dye) or TGA measurements (less selective and precise and having the drawback of not being applicable to the standard electrodes) on powdered TiO_2 samples. For these reasons, indirect UV-Vis method was selected for extensive FFD studies on real samples (Section 2.4.3), but TGA measurements were also used for validation purposes on some relevant uptake conditions on *P25* powders (end of section 3.4.2).

2.4.1 Preliminary evaluations

UV-Vis analyses were performed on ***D5*** ethanol solutions at different concentrations to obtain a mean value of the molar extinction coefficient (ε) at $\lambda = 448$ nm of 35530 cm^{-1}, since in the literature the only reported value was measured in acetonitrile as solvent.[15] It is worth noting that the maximum number of ***D5*** molecules that can be theoretically grafted must not exceed the physical sorption limit of additional ***D5*** layers not directly bound to titania. To stay below this limit, the suitable amounts of ***D5*** and *P25* for the adsorption should range, using 10 ml of ***D5*** solution, from 1.0 to 5.0 10^{-4} M, when using amounts of *P25* ranging from 1.0 to 5.0 mg, respectively. In fact the indirect evaluation of dye uptake by UV-Vis measurements requires that the process consumes a significant (approximately not less than 0.1%, as estimated from molar extinction coefficient and used concentration of ***D5***) mole fraction of dye. To find the correct ranges of ***D5*** concentrations and *P25* amounts the following considerations were made: assuming the chemical formula of TiO_2 (anatase phase, density 4.23 g cm^{-3}), a spherical shape of the particles with an average diameter of about 20-25 nm (confirmed by Sherrer particle size analysis from grazing incidence XRPD data collected from titania-covered slides as detailed in figure SI-1 in ESI file and it comment), the weight of one sphere of *P25* is 3.1906 10^{-17} g and the surface available for the sorption per mg of *P25* results 6.14 10^{16} nm^2. Moreover as evaluated with MOLDRAW,[38] a molecule of ***D5*** bound to the sphere by the cyanoacetic group and with the diphenyl amino moiety, forming the outer part, covers approximately 0.5 nm^2.

The results obtained from this preliminary uptake experiments are reported in Table 3. In each experiment the amount of *P25* was put in contact with the ***D5*** solution for 16 hours at 25°C in a dark bottle in order to preserve the solution from the light. The results are expressed as number of ***D5*** molecules (abbreviated "molec" from now on) retained in batch conditions by 1.0 mg of *P25* and the unit is therefore "molec mg^{-1}". In the planned experiments the bottom and the top levels of the variation ranges of ***D5*** and *P25* (experiments 1-4) were selected; moreover, in order to evaluate the experimental error associated to the method, three replicates were performed with both variables fixed to the values corresponding to the centre of the ranges (experiments 5-7). The evaluated standard deviation associated to the methodology was $4.77 \cdot 10^{16}$ molec mg^{-1} and the measured differences in the quantity of grafted ***D5*** are therefore statistically significant.

Table 3. ***D5*** uptake on *P25* powders.

	***D5* (mM)**	***P25* (mg)**
1	0.1	1.0
2	0.5	1.0
3	0.1	5.0
4	0.5	5.0
5	0.3	2.5
6	0.3	2.5
7	0.3	2.5

The obtained data confirmed that the sorption is affected by both variables with a positive correlation (the amount of grafted ***D5*** increases as the amounts of both ***D5*** and *P25* increase) and allowed optimizing the experimental procedure.[§] It must be noted that recorded UV-Vis spectra of the ***D5*** concentrated solutions show that the wavelength of the absorption maximum has a bathochromic shift of about 20 nm, probably due to the attractive inter-molecular interactions, highlighted by XRD analysis, more likely to occur in concentrated solutions. In order to avoid these aggregation processes, the dispersant *CDCA* must be included in the real uptake experiments on titania powders (section 3.4.2) and slides (section 3.4.3).

2.4.2 ***D5*** *sorption on P25 powder*

2^3 FFD - P25 powder was used as the simplest possible model system. A Full Factorial Design was planned in order to investigate the effect of ***D5*** concentration, contact time (*t*) and concentration of the co-absorbent *CDCA*.[7] In order to investigate the principal and the interaction effects of the three variables a FFD 2^3 plan was performed and the 8 required experiments (exp. 1-8) are reported in Table 4; moreover three replicates of the central experiment (exp. 9-11) were performed at the beginning, in the middle and at the end of the FFD in order to check the analysis repeatability and to estimate the experimental error.

Table 4. Experimental data from 2^3 FFD on titania powders. + and – represent the highest and the lowest values of the variables.

Exp	***D5***	***t***	***CDCA***	***D5*** [a]	***t*** [b]	***CDCA*** [c]	***Uptake*** [d]
1	-	-	-	0.04	4.0	0.0	8.1
2	+	-	-	0.40	4.0	0.0	8.4
3	-	+	-	0.04	28.0	0.0	7.3
4	+	+	-	0.40	28.0	0.0	13.5
5	-	-	+	0.04	4.0	16.0	5.7
6	+	-	+	0.40	4.0	16.0	5.2
7	-	+	+	0.04	28.0	16.0	4.4
8	+	+	+	0.40	28.0	16.0	12.0
9	0	0	0	0.22	16.0	8.0	8.0
10	0	0	0	0.22	16.0	8.0	8.2
11	0	0	0	0.22	16.0	8.0	8.2

[a] mM [b] h [c] mM
[d] *D5* molecules mg^{-1} 10^{16}

The results reported in Table 4 were used to calculate an Ordinary Least Squares (OLS) regression model relating the experimental result "y", i.e. the amount of grafted ***D5***, to the experimental factors (***D5*** and *CDCA* concentrations and contact times) and to their interactions. The significant effects were evaluated by a *Student t test* where each regression coefficient was compared with the standard error multiplied by the proper *t* value of 2.92 (α = 95%, 3 degrees of freedom).

The following OLS model was obtained for ***D5*** uptake by powdered titania (molec $mg^{-1}10^{16}$), i.e "*Yp"* the following equation:

$Yp = 8.11 + 1.69\boldsymbol{D5} + 1.24t - 1.25CDCA + 1.73\boldsymbol{D5}\,t$ Eq. 1

which resulted satisfactory since the R^2 value was 0.9914 and, as shown in the ESI file (figure SI-5a), the observed and predicted values are in good agreement.

The OLS model indicates the relevant factors and their effects on the amount of adsorbed ***D5****:* the higher the value of the coefficient in each term, the more important the factor in affecting the response and a "plus" or "minus" sign indicates an increase or a decrease of the ***D5*** uptake when the considered factor is increased. All the principal factors are relevant from statistical analysis of experimental data: ***D5*** and *t* are both associated to a positive effect, while on the contrary *CDCA* has a negative effect, i.e larger *CDCA* concentrations hamper high uptakes. Nevertheless, for the comprehension of the system, the effects of the interaction factors, when relevant, must be considered. In fact they allow describing the simultaneous effects that the factors exert on the system in either a synergic or in an antagonistic way. In our case only the interaction effect between ***D5*** and *t* is relevant; a graphical method based on a two-way table is the best approach to highlight their mutual interaction.

The two-way table (Figure 5) is built by averaging the response of each couple of combinations with the same values of the two variables: on the rows there are the ***D5*** concentration values and on the columns the soaking time values (*t*), so the bottom left quadrant represents the experiments of plan characterized by the lowest ***D5*** value (-) and the lowest *t* value (-); since there are two experiments with these values (i.e. experiments 1 and 5) the average of the responses given by two experiments is reported in the table.

D5 **uptake** (molec mg^{-1} 10^{16})			
D5 (mM)	0.40	6.8	12.7
	0.04	6.9	5.9
		4.0	28.0

	t *(*h*)*

Figure 5: Two-way table illustrating the *D5*t* two factor interaction.

In the bold central cell, moving from left to right corresponds to keeping the ***D5*** concentration constant (and vary the time *t* from the lowest to the highest value), conversely by moving from bottom to top *t* remains constant and the ***D5*** concentration increases.

On one hand ***D5*** and *t* show a synergistic effect, since the largest values of dye uptake were obtained, as expected, when high concentrations of ***D5*** were put in contact for long time (top right corner). In this condition the synergistic effect is dominant also with respect to the *CDCA* addition, since no relevant variations in the amount of dye uptake were recorded in the experiments with or without the dispersing agent (see experiments 4 and 8 in Table 4). On the other hand both intermediate conditions (long soaking time and low ***D5*** concentration or short soaking time and high ***D5*** concentration) reduce ***D5*** uptake with respect to low ***D5*** concentration and short *t* (down left corner).

In these experiments the *F test*[39] for the presence of the quadratic effect resulted negative, so performing additional experiments to evaluate further variable levels, besides the three chosen ones, would not add any new information about the studied system.

The adopted method can measure precisely, but in an indirect way, the amount of dye extracted from the solution by titania powders and slides. The method was validated by evaluating the quantity of grafted dye also by TGA measurements, which have the advantage of directly detecting the uptaken amounts, but the drawback of being less precise and not applicable to slides used in technological applications.

Thermogravimetric analyses (TGA) - TGA analyses were carried out in air on ***D5***, *CDCA* and pure TiO_2 powder as reference materials (Figure SI-6a), then on ***D5***-sensitized TiO_2 powders with and without *CDCA* in the same conditions of the experiments 4 (+ + -) and 6 (+ - +) (Table 2), corresponding to highest uptake in absence and presence of *CDCA* respectively (Figure SI-6b). Full TGA data plots and comments are available in the ESI file. UV-Vis indirect determination indicated an uptake of 1.0 10^{17} molecules of ***D5*** for 3.0 mg of *P25*. Taking into account the molecular weight of ***D5***, this corresponds to an expected weight loss of 2.7%. TGA data indicated for the two analyzed samples a weight loss between 3 and 6%, depending on the adsorption conditions. These values are in agreement with the previous determination (same order of magnitude of the UV-Vis) and confirm that the dye that is left in the solution, precisely detected by UV-Vis measurements, was actually grafted on the TiO_2 powder.

As shown in the ESI file (figure SI-6), the plots of *P25* and ***D5***-sensitized *P25* are significantly different. A first consideration, confirming a chemical interaction between the dye and the substrate, is the clear difference in the thermal degradation profile shown by pure ***D5*** with respect to the ***D5***-sensitized sample. This suggests that the effect of the contact does not originate a physical mixture, but instead, a system with strong interfacial interactions, able to significantly modify the thermal degradation profile.

While pure *P25* shows a total weight loss of 1.4%, with a significant contribution due to physisorbed water desorption, ***D5***-sensitized sample has a lower weight residue due to the decomposition of the organic dye, leading to a final weight loss of 7.4%.

In order to quantify the amount of dye in the sample, a weight loss contribution of *P25* similar to the neat material (1.4%) should be assumed and subtract from 7.4% obtaining 6.0%. Since ***D5*** degrade only for the 95.9% of their initial weight the neat weight loss due to ***D5*** can be estimated about of 6.3% of the total weight of the sample.

The estimated value of adsorbed ***D5*** molecules per gram of *P25* from these measurements results $9.0*10^{19}$ Molec $gram^{-1}$. This result is consistent with the indirect Uv-Vis measurements and demonstrates that the main mechanism of dye removal from the contact solution is due to adsoption onto the *P25*.

In presence of *CDCA* during the dye uptake, the TGA profile shows an higher weight loss and a slight shift of all the degradation processes at lower temperatures. The onset of the degradation process (appearing above 200°C) is anticipated of about 20°C with respect to *D5-P25* system (observed at 220°), and the maximum of degradation rate is anticipated of about 9°C. Compared with ***D5***-sensitized *P25*, the additional weight difference (0.68%) suggested the presence of *CDCA* co-grafted with ***D5*** in the sample. An approximate 1:10 ratio between *CDCA* and ***D5*** onto TiO_2 surface can be estimated from this experiment.

*2.4.3 **D5** sorption on TiO_2 commercial slides*

After the successful experiment on *P25* powders, an analogous FFD 2^3 plan was performed on TiO_2 commercial slides in order to investigate the principal and the interaction effects of the three variables, in the real working conditions. Each experiment consists of a sorption test in which the TiO_2 slides are immersed in 10.0 mL of a solution containing ***D5*** and *CDCA* at the different concentrations and for the contact times required by the experimental plan. Three replicates of the central experiment (Exp. 9-11) were performed at the beginning, in the middle and at the end of the FFD in order to check the analysis repeatability and to estimate the experimental error. The eight required experiments (exp. 1-8) plus three repetitions of the central point are reported in Table 5, where uptake is expressed, differently from experiments with titania powders, as the number of uptaken molecules in the unit volume of TiO_2 (molec cm^{-3}). This unit was chosen because is the more direct from the technologic application viewpoint and because is impossible an accurate evaluation of the weight of TiO_2 film on slides. Uptake

values in this unit can be calculated, knowing the thickness of the slides (6.5 ± 0.4 μm), which is homogeneous within this experimental error (see experimental section for details). This homogeneity allows to compare the data from different slides and transform the amount of grafted molecules from molec cm^{-2} of slide (the quantity used for technological applications) to molec cm^{-3} of TiO_2 (used in the TiO_2 slide experiments) and molec per weight unit of titania (molec mg^{-1}) used in the powder experiment. It is worth nothing that the large apparent differences in table 4 and 5 (3 order of magnitude) is due to the different measurement units.

Exp	***D5***	***t***	***CDCA***	***t*** *[a]*	***D5*** *[b]*	***CDCA*** *[c]*	***Uptake*** *[d]*
1	**-**	**-**	**-**	8.0	0.05	0.0	4.0
2	**+**	**-**	**-**	24.0	0.05	0.0	3.5
3	**-**	**+**	**-**	8.0	0.50	0.0	56.3
4	**+**	**+**	**-**	24.0	0.50	0.0	35.7
5	**-**	**-**	**+**	8.0	0.05	16.0	5.3
6	**+**	**-**	**+**	24.0	0.05	16.0	6.3
7	**-**	**+**	**+**	8.0	0.50	16.0	51.3
8	**+**	**+**	**+**	24.0	0.50	16.0	60.8
9	0	0	0	16.0	0.27	8.0	29.1
10	0	0	0	16.0	0.27	8.0	28.9
11	0	0	0	16.0	0.27	8.0	29.2

Table 5. Experimental data from 2^3 FFD on titania-covered slides

[a] h; [b] mM; [c] mM;
[d] *D5* molecules cm^{-3} 10^{19}.

From these results the following OLS model was obtained for ***D5*** uptake by titania slides (Molec cm^{-3} * 10^{19}), i.e "*Ys"* in the following equation:

$$Ys = 28.2 + 23.1\ \mathbf{D5} + 3.0\ CDCA + 3.96\ t \cdot CDCA + 2.0\ \mathbf{D5} \cdot CDCA + 3.6\ t \cdot \mathbf{D5} \cdot CDCA \qquad \text{Eq. 2}$$

which resulted satisfactory (R^2 = 0.9850); also in this case the observed and predicted values are in good agreement (see ESI, Figure SI-5b).

D5 and *CDCA* are the only principal relevant factors and are both associated to a positive effect, contrary to titania powder FFD (see q. 1) where *CDCA* has negative effect. Moreover the interactions of two and three factors are relevant. Also in this case the information contained in the three factor interaction can be efficiently extracted and shown by a graphical method considering the three possible two way tables (see previous section for their detailed definition), constructed using the variation of the experimental response when varying each time a couple of factors, while leaving the third factor constant.

From the data of Figure 6 it is clear that, when ***D5*** concentration is high (see the left part of the figure), it is possible to obtain large ***D5*** uptakes in many different situations (i.e. at low contact time in absence of *CDCA*, 56.3 molec cm^{-3} 10^{19}, or even in the presence of high concentration *CDCA* if the contact time is high, 60.8 molec cm^{-3} 10^{19}). This behaviour can be explained with the polydispersity of the titania substrate presenting a distribution of adsorption sites. At shorter times and without *CDCA*, kinetic effects prevail and less stable and more accessible sites are saturated. Conversely at longer times thermodynamic equilibrium is reached, saturating stable sites with a partial bleaching of less stable sites.

When ***D5*** is at low values (see the right part of the Figure 6) the best result was obtained when *CDCA* and *t* are high, but the grafted amounts are very small and comparable to the experimental error, so the recorded variations cannot be considered statistically significant; the same considerations can be done about the other two way tables (see Figure SI-7). Also in this case, the evaluation of the second order effect, with the addition of further variable levels to be investigated, was not required since the *F-test* for the presence of the quadratic effect resulted negative[39].

		D5 **uptake (molec cm^{-3} 10^{19})**		***D5*** **uptake (molec cm^{-3} 10^{19})**	
		D5 at high value		*D5* at low value	
CDCA	16.0	51.3	60.8	5.3	6.3

(mM)	0.0	56.3	35.7	4.0	3.5
		8.0	24.0	8.0	24.0
		t (h)		***t*** (h)	

Figure 6: Two-way table illustrating the ***D5****CDCA*t* three factor interaction: here only the table obtained for ***D5*** fixed at high and low values is presented, the other two tables (for fixed values of *CDCA* and *t*) are reported in the Supplementary Information (Figure SI-7).

The higher uptake conditions at the most interesting cases of high ***D5*** concentrations can also be clearly seen in Figure 7 visualizing in three dimensions the data of Figure 6.

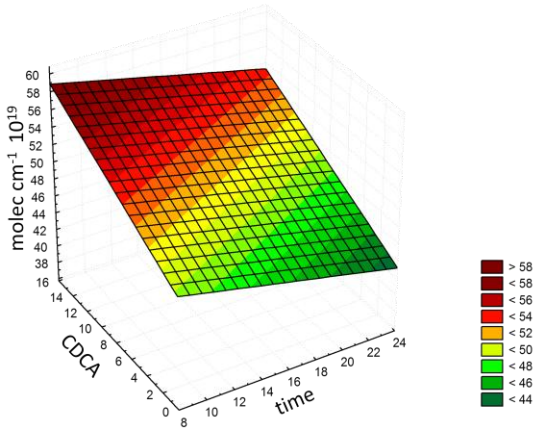

Figure 7. Surface plot illustrating the three-factor interaction ***D5****CDCA*t* interactions, obtained for ***D5*** at fixed high concentration, constructed from the two way tables. The other two interactions (for fixed values of *CDCA* concentration and *t*) are reported in the ESI file in tabular format (Figure SI-7).

The different effect of *CDCA* on TiO_2 slides and on TiO_2 powder can be explained by the different diffusion conditions and available space for the ***D5*** molecules in the two samples. In fact in the powder sample, the TiO_2 nano-particles are suspended in the solvent with no diffusion limitations and are easily accessible to ***D5***. At the same time at concentration of the order of 10^{-4} M, ***D5*** molecules are well diluted and far away one from the other and aggregation effects are limited either in presence or in absence of *CDCA*. On the contrary on slide samples, when ***D5*** molecules approach the TiO_2 slide surface and start penetrating into the interstitial space among the nano-particles of the TiO_2 layer, the available space is much smaller, diffusion became a limiting step, with a compromise between kinetic and thermodynamic effects (as discussed before commenting figure 6). ***D5*** molecules are then constrained one close to the others, thus facilitating the formation of dimers and aggregates induced by the interactions unraveled by XRD and calculations. In this situation, the *CDCA* action as dispersant becomes important to optimize the dye uptake, especially at high concentrations and for long soaking times, both factors able to induce aggregation. Understanding the driving forces of the aggregation processes by structural and molecular interactions analyses was then of paramount importance for the interpretation of the dye uptake results, as summarized in the following section.

3. Discussion on combined approach

The structures obtained from XRD show the most stable conformations suggested by the calculations on the isolated molecules. This implies that the intermolecular interactions dictating crystal packing are not strong enough to vary the thermodynamically stable conformations. Several weak interactions, besides the expected H-bonds, were observed in the three structures, all showing close contacts between the phenyl moieties. The ***D5*** precursor, molecule **4**, showed *T*-like interactions between thiophene groups, while ***D5*** showed parallel packing of the aromatic moieties. These two kinds of stacking are also probable on the TiO_2 surface with no definite preference for one of the two arrangements. It can be inferred that the same interactions must play an important role and induce aggregation of ***D5*** related molecules in solution and on the titanium oxide surface. These aggregation forces can explain the well known dispersion problems shown by ***D5*** and by ***D5*** on TiO_2 surface, i.e, self absorption and lateral charge transfer between different dye molecules, with reduction of the injection yields.

The information on the energy barriers suggests that preparation and soaking conditions allow the co-existence (in solution and on the surface) of a variety of conformers even different from the most stable ones. Moreover, the electron injection yield during DSC functioning can be in principle conformer-dependent, since the different conformations show different planarity and the electronic conjugation along the ***D5*** framework is modified. A computational study of the excited state structure, taking into account both flexibility and conformational freedom, might provide more insight on the “real world”.

X-ray diffraction and calculations gave interesting indications of the structure of ***D5*** in different situations, but could not evaluate the importance of the disaggregating agent (*CDCA*) and the influence of time of soaking, concentration of reagents, physical form of titania (powder or slide) on the dye uptake mechanism. The spectroscopy measurements, aided by a chemometric approach to reduce the number of experiments and investigate the interactions between the various parameters influencing dye uptake, allowed answering some of the issues where XRD could not provide insights.

The Full Factorial Design indicated, at first, that titania powder and titania slides behave differently (*CDCA* role is relevant only in TiO_2 slides, see Figure 6), likely due to the larger importance of diffusion problems in the solid sintered thin film. Therefore, among the studied models, the reference one must be the one carried out on TiO_2 slides. In this case, time and *CDCA* concentration are antagonist, meaning that the presence of *CDCA* allows a large dye uptake only at long soaking times,

while good uptakes can be obtained at low soaking times and no *CDCA*. These two situations both allow large uptakes, but with long soaking times and with *CDCA* a uniform titania sparse loading is obtained, as suggested by high injection yields,[7,14] while with short soaking time and no *CDCA* ***D5*** aggregation and island formation probably occurs on the titania surface.

4. Conclusions

First principle calculations, X-ray diffraction, UV-Vis spectroscopy, TGA and DoE techniques have been used in a synergic way to shed light on the destiny of dye molecules before, during and after the grafting process on TiO_2 electrodes. DSC key components, i.e. dye and titania, have been studied from the viewpoints of the molecular structure and of the dye uptake mechanism, using the well-known ***D5*** molecule as a case study. This combined characterization approach provided at first a detailed information about the molecular interactions, stable conformations and flexibility of the dye molecules. R-PES calculations, besides facilitating structure solutions by powder diffraction, suggested that dyes can exploit their conformational flexibility to optimize the grafting and packing on TiO_2 surface, with a wider then expected available conformational landscape. These data are fundamental to better understand, in working conditions, the role of *CDCA* and the optimized uptake conditions of ***D5*** on a TiO_2 slides. In fact the ability of *CDCA* in modifying dye uptake (DoE), i.e. that of hindering phenyl-phenyl intermolecular contacts and contrast the *T*-like and parallel stacking (X-ray), by intercalating on TiO_2 (TGA) between adjacent ***D5*** molecules, is clarified by the quantitatively measuring (UV-Vis) of the parameters involved in dye uptake.

The DoE-assisted spectroscopic investigation was applied to evaluate the dye uptake in DSC. The successful interpretation of the obtained model, carried out by the complementary characterization techniques, allowed us to propose the presented UV-Vis/DoE approach as the simplest, fastest, most reproducible and sensitive method that can be widely applied to understand and optimize the uptake of any kind of dye.

Experimental Section

Materials

TiO_2 (Degussa *P25*, purity 99.5%) (Germany), ethanol (purity 99.8%) and cheno-deoxycholic acid (*CDCA*) (>97%) were purchased from Sigma-Aldrich (Sigma-Aldrich (Milwaukee, WI, USA). Glass slides covered with TiO_2 were purchased from DyeSol Italia (Roma, Italy). The ***D5*** stock solution was prepared at 5.0 10^{-4} M by dissolving 0.0445 g in 200.0 mL of ethanol; working solutions at different concentrations were obtained by dilution with ethanol of the stock solution.

Synthesis

Full details on synthesis of compounds 3, **4**, ***D5*** and **6** are available in the ESI file section 1.

Instrumentation

1H- and 13C-NMR spectra were recorded on a Avance-200 instrument (Bruker, Milan, Italy) operating at 200 MHz and 50 MHz respectively and ESI-MS spectra were recorded using a LCQ Deca XP plus spectrometer (ThermoElectron Corporation, Rodano, MI, Italy) as detailed in ESI file, section 1. UV-Vis data were collected by a UV-Vis Lambda 900 spectrophotometer (Perkin-Elmer, Monza, MI, Italy). TGA measurements were collected on a TGA/DTA LF1100/851e, equipped with Store Software (Mettler Toledo, Novate Milanese, MI, Italy) instrument, using the following standard conditions: equilibration step at 60°C for 30 minutes, followed by a ramp at 10°C/min rate up to 800°C. Measurements were collected under air flow. X-ray powder diffraction measurements to analyze TiO_2 particle size were performed on a ThermoARL powder diffractometer XTRA and the details are given in the ESI file.

Single-crystal diffraction data were collected using an Oxford Xcalibur CCD area detector diffractometer with graphite monochromator and Mo-Kα (λ =0.71069 Å) radiation. Data reduction and absorption corrections were performed using CrysAlisPRO 171.34.44 (Agilent Technologies, Cernusco, MI, Italy). Single crystal structure solution was performed by direct methods using SIR2011[40] and refinement with full-matrix least-squares employing SHELX-97.[41] Hydrogen atoms were generated in calculated positions by SHELX-97. Single crystals of compounds **4** and **6**, suitable for X-ray analysis were both obtained by slow cooling of a saturated hot ethanol solution. Attempts at growing ***D5*** crystals from different solvents and different temperature conditions only yielded too small micron-size crystals and powder diffraction experiment had to be performed instead, using the micro-crystals grown in acetonitrile. Relevant crystal data are reported in the ESI file. X-ray powder diffraction (XRPD) experiments were performed at the ESRF in Grenoble on the BM1A and BM1B beamlines, using a high resolution powder diffraction instrument (used for indexing) and a Pilatus 2M detector[42] placed at a distance of 120 cm at two different height with respect to incoming X-ray beam to get low and high 2θ angular range (used for structure solution). The Pilatus XRPD patterns were collected using radiation with λ = 0.7040 (1) Å. The calibration was done using the lattice parameters of the NIST Lanthanum Hexaboride (LaB6) standard (SRM 660b; nominal a = 4.15695(6) Å at RT). The crystal structure was solved from powder diffraction data by simulated annealing using the low angle dataset only by EXPO2011 software.[43] The two powder patterns, at low and high 2θ range, were refined together by the Rietveld method using the TOPAS software.[44] Full details on crystallographic measurements are reported in ESI file.

Theoretical calculations

The structural models of ***D5*** were obtained by first principle DFT calculations employing the G03[45] software, as detailed in the computational section. A careful analysis of stable energy minima and of the energy barriers separating them was carried out by using the B3LYP[46] functional and different basis sets depending the size of calculations, as detailed on the result sections.

Determination of D5 uptake

Sorption experiments were carried out by adding, in static conditions, the proper amounts of ***D5*** to the selected amounts of *P25* powder for each experiment. The systems were electromagnetically stirred for a total time of 16 hours; then 1.00 mL of the supernatant is collected, centrifuged twice at 26°C, 3000 rpm for 15.0 min, filtered on 0.20 μm polypropylene membrane (VWR International, West Chester, PA, USA). UV-Vis analysis was performed at 447.9 nm for the determination of the amount of dye still present in solution. All solutions were maintained in the dark.

The particle size and film thickness of the transparent TiO_2 covered glass (named "TiO_2 slides"), purchased by Dyesol, were characterized by XRPD and UV-Vis-NIR spectroscopy respectively, as detailed in Figure SI-1 and SI-2 and their caption. A particle size of about 25 nm and a thickness of the TiO_2 film of 6.5±4 μm was detected. These values were used to calculate the amount of available grafting sites and to estimate the amount of ***D5*** that can be adsorbed by a single slide for a better design of the preliminary experimental plan. The TiO_2 thickness was checked by NIR measurements (see ESI, Figure SI-2 and Table SI-1 and its comment), analyzing the absorption interference fringes of the TiO_2 slides, generated by the similarity of the radiation wavelength and the TiO_2 thickness.[47]

The transparent TiO_2 slides were immersed, in static conditions in a beaker, in 10.00 mL of the different solutions containing the different amounts of ***D5*** and cheno-deoxycholic acid (*CDCA*) and for the contact times dictated by the DoE. Concentrations and contact times are usually optimised by trial and error method. Typical literature[7-14] conditions are 1-0.1 mM for ***D5***, 10 mM for *CDCA* and 16 h contact time (overnight). Their values were chosen for the DoE to explore the variable space and find the optimal soaking condition.

Then the supernatant was collected, filtered and analyzed by UV-Vis (447.9 nm) for the determination of the amount of dye still present in solution. All the solutions were maintained in the dark.

The *P25* powder and TiO_2 slides were washed after the sorption experiments by two 10.00 mL aliquots of ethanol; the aliquots were then recovered, centrifuged, filtered and analyzed by UV-Vis in the same conditions of the sorption experiments.

Chemometric analysis

Full Factorial Design, regression models and all graphical representations were performed by Statistica 7.1 (Statsoft Inc., U.S.A.) and Excel 2003 (Microsoft Corporation, U.S.A.).

Acknowledgements

We would like to thank A. Coelho (Coelho Software Brisbane, Australia) for his advice and especially for the use of constraints in the TOPAS program. Prof. Davide Viterbo is acknowledged for useful suggestions and discussion during data analysis and manuscript preparation. ESRF and SNBL are acknowledged for beam time. D. Chernyshov (SNBL, Grenoble, FR) is acknowledged for support in data collection and reduction of XRPD Pilatus 2M data. Fondazione CRC (grant n. 2008-1581) is gratefully acknowledged for funding. L.P. acknowledges financial contributions by the MIUR project "Multidisciplinary modeling of the structure of layered materials" funded as FIRB in 2012, (code RBFR10CWDA) for funding his bursary. C.B.and V.G. gratefully acknowledge financial support by DSSCX project (PRIN 2010-2011, 20104XET32) from Ministero dell'Istruzione, dell'Università e della Ricerca. Finally G.F. thanks the "Scuola di Alta Formazione" of the University of Piemonte Orientale (Italy) and Compagnia di San Paolo for funding her PhD bursary.

Keywords: DSC • Dye uptake • Chemometrics • UV-Vis Spectroscopy • X-ray Powder Diffraction

[1] a) M. Grätzel, *Acc. Chem. Res*., **2009**, *42*, 1788-1798; b) A. Hagfeldt, G. Boschloo, L. Sun, L. Kloo, H. Pettersson, *Chem. Rev.*, **2010**, *110*, 6595-6663; c) J. Burschka, N. Pellet, S.J. Moon, R. Humphry-Baker, P. Gao, M.K. Nazeeruddin, M. Graetzel, *Nature*, **2013**, *499*, 316-319.

[2] H.S. Jung, JK Lee, *J. Phys. Chem. Lett.*, **2013**, *4*, 1682-1693.

[3] R. Y. Ogura, S. Nakane, M. Morooka, M. Orihashi, Y. Suzuki, K. Noda, *APL 94*, **2009**, 073308

[4] For comprehensive reviews, see: a) H. Imahori, *T*. Umeyama, S. Ito, *Acc. Chem. Res*., **2009**, *42*, 1809-1818; b) A. Mishra, M. K. R. Fischer, P. Bauerle, *Angew. Chem., Int. Ed.,* **2009**, *48*, 2474-2499;c) J.N. Clifford, M. Planells, E. Palomares, *J. Mater. Chem.,* **2012**, *22*, 24195-24201; d) J. Park, G. Viscardi, C. Barolo, N. Barbero, *Chimia*, **2013**, *67*, 129-135; for some selected recent examples: e) A. Yella, H.-W. Lee, H. N. Tsao, C. Yi, A. K. Chandiran, M. K. Nazeeruddin, E. W.-G. Diau, C. Y. Yeh, S. M. Zakeeruddin, M. Grätzel, *Science*, **2011**, *334*, 629-634; f) J. Park, C. Barolo, F. Sauvage, N. Barbero, C. Benzi, P. Quagliotto, S. Coluccia, D. Di Censo, M. Grätzel, Md. K. Nazeeruddin, G. Viscardi *Chem. Commun.,* **2012**, *48*, 2782-2784; g) C. Barolo, J-H Yum, E. Artuso, N. Barbero, D. Di Censo, M. G. Lobello, S. Fantacci, F. De Angelis, M. Grätzel, Md K Nazeeruddin, G. Viscardi, *Chem.Sus.Chem*, **2013**, *6*, 2170–2180.

[5] N. Cai, R. Li, Y. Wang, M. Zhang, P. Wang, *Energy Environ. Sci.*, **2013**, *6,* 139-147.

[6] a) B. O'Regan,L. Xiao, *T*. Ghaddar, *Energy Environ. Sci.*, *2012*, **5**, 7203-7215; b) V. Johansson, L. Ellis-Gibbings, *T*. Clarke, M. Gorlov, G. G. Andersson, L. Kloo, *Phys. Chem. Chem. Phys.*, **2014**, 16, 711-718.

[7] D.P. Hagberg, J.-H. Yum, H.J. Lee, F. De Angelis, *T*. Marinado, K. M. Karlsson, R. Humphry-Baker, L. Sun, A. Hagfeldt, M. Grätzel, Md. K. Nazeeruddin, *J. Am. Chem. Soc.* **2008**, *130,* 6259-6266.

[8] E. Ronca, M. Pastore, L. Belpassi, F. Tarantelli, F. De Angelis, *Energy Environ. Sci.*, **2012**, *6*, 183-193.

[9] M. Pastore, E. Mosconi, F. De Angelis, M. Grätzel, *J. Phys. Chem. C* **2010**, *114,* 7205-7212.

[10] F. Labat, *T*. Le Bahers, I. Ciofini, C. Adamo, *Acc Chem Res*, **2012**, *45*, 1268-1277.

[11] E. Dell'Orto, L. Raimondo, A. Sassella, A. Abbotto, *J. Mater. Chem.*, **2012**, *22*, 11364-11369.

[12] H.-P. Lu, C.-Y. Tsai, W.-N. Yen, C.-P. Hsieh, C.-W. Lee, C.-Y. Yeh, E.W.-G. Diau, *J. Phys. Chem.*, **2009**, *113*, 20990-20997.

[13] J. Li, W.J. Wu, J.B. Yang, J. Tang, Y.*T*. Long, J.L Hua, *Science China Chem.*, **2011**, *54*, 699-706.

[14] D.P. Hagberg, *T*. Edvinsson, *T*. Marinado, G. Boshloo, A. Hagfeldt, L. Sun, *Chem. Commun.,* **2006**, 2245-2247.
[15] G. Boschloo, *T*. Marinado, K. Nonomura, *T*. Edvinsson, A. G. Agrios, D. P. Hagberg, L. Sun, M. Quintana,C. S. Karthikeyan, M. Thelakkat, A. Hagfeldt, *Thin Solid Films*, **2008**, *516*, 7214-7217.
[16] a) W. Zeng, Y. Cao, Y. Bai, Y. Wang, Y. Shi, M. Zhang, F. Wang, C. Pan, P. Wang, *Chem. Mater.*, **2010**, *22*, 1915-1925; b) H.N. Tsao, J. Burschka, C. Yi, F. Kessler, M.K. Nazeeruddin, M. Grätzel, *Energy Environ. Sci.*, **2011**, *4*, 4921-4924; c) H. N. Tsao, C. Yi, *T*. Moehl, J.-H. Yum, S. M. Zakeeruddin, M. K. Nazeeruddin, M. Grätzel, *ChemSusChem*, **2011**, *4*, 591–594; d) M. Xu, M. Zhang, M. Pastore, R. Li, F. De Angelis, P. Wang, *Chem. Sci.*, **2012**, *3*, 976-983.
[17] R. Gobetto, C. Nervi, B. Romanin, L. Salassa, M. Milanesio, G. Croce, *Organometallics*, **2003**, *22*, 4012-4019.
[18] A. Arrais, E. Diana, R. Gobetto, M. Milanesio, D. Viterbo, P. L. Stanghellini, *Eur. J. Inorg. Chem.*, **2003**, *6*, 1186-1192.
[19] A. Arrais, E. Boccaleri, G. Croce, M. Milanesio, R. Orlando, E. Diana, *Cryst. Eng. Comm.*, **2003**, *5*, 388-394.
[20] R. Gobetto, G. Caputo, C. Garino, S. Ghiani, C. Nervi, L. Salassa, E. Rosenberg, J. B. A. Ross, G. Viscardi, G. Martra, I. Miletto, M. Milanesio, *Eur. J. Inorg. Chem.*, **2006**, *14*, 2839-2849.
[21] F. H. Allen, *Acta Cryst.*, **2002**, *B58,* 380-388.
[22] a) S. P. Anthony, C. Delaney, S. Varughese, L. Wang, S. M. Draper, *Cryst. Eng. Comm*, **2011**, *13*, 6706-711; b) S. P. Anthony, S. Varughese, S. M. Draper, *Chem. Commun.*, **2009**, 7500-7502; c) S.P. Anthony, S. Varughese, S.M. Draper, *J. Phys. Org. Chem.*, **2010**, *23*,1074-1079.
[23] a) Y.-*T*. Li, C.-L. Chen, Y.-Y. Hs, H.-C. Hsu, Y. Chi, B.-S. Chen, W.-H. Liu, C.-H. Lai, *T*.-Y. Lin, P.-*T*. Chou, *Tetrahedron*, **2010**, *66*, 4223-4234; b) S. Zheng, S. Barlow, C. Risko, *T*. L. Kinnibrugh, V. N. Khrustalev, S. C. Jones, M. Yu. Antipin, N. M. Tucker, *T*. V. Timofeeva, V. Coropceanu, J.-L. Bredas, S. R. Marder, *J. Am. Chem. Soc.*, **2006**, *128*, 1812-1817; c) F.-R. Dai, W.-J. Wu, Q.-W. Wang, H. Tian, W.-Y. Wong, *Dalton Trans.*, **2011**, *40*, 2314-2323.
[24] E. M. J. Johansson, *T*. Edvinsson, M. Odelius, D. P. Hagberg, L. Sun, A. Hagfeldt, H. Siegbahn, H. Rensmo, *J. Phys. Chem. C,* **2007**, *111*, 8580-8586.
[25] G. E. P. Box, W. G. Hunter, J. S. Hunter, *Statistic for experimenters*. Wiley, New York, **1978**.
[26] R. Carlson, *Design and optimisation in organic synthesis*. Elsevier, Amsterdam, **1992**.
[27] S. N. Deming, S. L. Morgan, *Experimental design: a chemometric approach*. Elsevier, Amsterdam, London, New York, Tokyo, **1993**.
[28] a) F. Bella, D. Pugliese, J. R. Nair, A. Sacco, S. Bianco, C. Gerbaldi, C. Barolo, R. Bongiovanni, *Phys. Chem. Chem. Phys.*, **2013**, *15*, 3706-3711; b) D. Pugliese, F. Bella, V. Cauda, A. Lamberti, A Sacco, E. Tresso, S. Bianco, *ACS Appl. Mater. & Interfaces*, **2013**, *5*, 11288-11295.
[29] Y. J. Cheng, J. Luo, S. Hau, D. H. Bale, *T*.-D. Kim, Z. Shi, , D.-B. Lao, N. M. Tucker, Y. Tian, L. R. Dalton, P. J. Reid, A. K. Y. Jen, *Chem. Mater.* **2007**, *19*, 1154-1163.
[30] H. Xia, J. He,; B. Xu, S. Wen, Y. Li, W. Tian, *Tetrahedron*, **2008**, *64*, 5736-5742.
[31] L. J. Gooßen, J. Paetzol, L. Winkel, *Synlett*, **2002**, *10*, 1721-1723.
[32] J. W. Hagemann in *Crystallization and Polymorphism of Fats and Fatty Acids*, (Eds.: N. Garti, K. Sato), Marcel Dekker Inc: New York and Basel, **1988**, pp. 9-96.
[33] M. P. Balanay, S.-M. Kim, M. J. Lee, S. H. Lee, D. H. Kim, *Bull. Korean Chem. Soc.*, **2009**, *30*, 2077-2082.
[34] L. Palin, C. Barolo, D. Chernyshov, D. Viterbo, A.G. Moliterni, G. Croce, W. van Beek, M. Milanesio, Data collection and analysis strategies for structure solution of complex organic structures, in preparation for submission to *J. Appl. Cryst*
[35] M. Milanesio, P. Ugliengo, D. Viterbo, G. Appendino, *J. Med. Chem.*, **1999**, *42*, 291-299.
[36] V. Gianotti, M. Benzi, G. Croce, P. Frascarolo, F. Gosetti, E. Mazzucco, M. Bottaro and M.C. Gennaro, *Chemosphere*, **2008,** *73*, 1731-1736.
[37] S. Polati, F. Gosetti, V. Gianotti, M.C. Gennaro, *J. Environ. Science and Health B*, **2006**, *41*, 765-779.
[38] a) P. Ugliengo, D. Viterbo, G. Chiari, *Z. Krist.*, **1993**, *207*, 9-23; b) Web Site: http:/www.moldraw.unito.it.
[39] A. I. Khuri, J. A. Cornell, *Response Surface, Design and Analysis*, Marcel Dekker, New York, **1987**.
[40] M. C. Burla, R. Caliandro, M. Camalli, G. L. Cascarano, C. Giacovazzo, M. Mallamo, A. Mazzone, G. Polidori, R. Spagna, *J. Appl. Cryst.*, **2012**, *45*, 357-.
[41] G.M. Sheldrick *Acta Cryst. A*, **2007**, *64*, 121.
[42] B. Henrich, A. Bergamaschi, C. Broennimann, R. Dinapoli, E.F. Eikenberry, I. Johnson, M. Kobas, P. Kraft, A. Mozzanica, B. Schmitt, *Nucl. Instr. and Meth. A*, **2009**, *607*, 247-.
[43] a) EXPO2011, version 1.12.09a, http ://www.ba.cnr.it; b) A. Altomare, M. C. Burla, G. Cascarano, C. Giacovazzo, A. Guagliardi, A. G. G. Moliterni, G. Polidori, *J. Appl. Cryst.*, **1995**, *28*, 842-846; c) A. Altomare, G. Cascarano, C. Giacovazzo, A. Guagliardi, M. C. Burla, G. Polidori, M. Camalli, *J. Appl. Cryst.*, **1994**, *27*,435-436.
[44] A. A. Coelho, *J. Appl. Crystallogr.*, **2005**, *38*, 455-461; A. A. Coelho *J. Appl. Crystallogr.*, **2003**,*36*, 86-95
[45] M. J. Frisch, et al. Gaussian 03, Revision C.02, Gaussian, Inc., Wallingford CT, **2004**.
[46] a) A. D. Becke, *J. Chem. Phys.*, **1993**, 98, 5648-5652; b) C. Lee, W. Yang, R.G. Parr, *Phys. Rev. B*, **1988**, *37,* 785-789
[47] a) M. Caglar, Y. Caglar, S. Ilican, *J. Optoelectr. Adv. Mater.*, **2006**, *8*, 1410-1413; b) S. Ilican, M. Caglar, Y. Caglar *Materials Science-Poland*, **2007**, *25*, 709-718.

* The crystal structures of ***D5***, **4** and **6** were submitted to the CCDC data centre with submission codes CCDC-953631 CCDC-895122 and CCDC-895123. These data can be obtained free of charge from The Cambridge Crystallographic Data Centre via www.ccdc.cam.ac.uk/data_request/cif.

‡ The Design of Experiments (DoE) is based on model systems of different complexity in order to obtain the evaluation and control of the investigated variables in the appropriate variation ranges. In general the exploration of the experimental domain starts with a two level full factorial design (FFD), allowing the study of the effects of the principal factors and of their interactions on the investigated response. The number of experiments required is 2p, p being the number of investigated factors. These experiments correspond to all the possible combinations of the two levels (usually indicated with + and -) of the considered factors; then, if necessary, other experiments are added in order to study the second order effects of the investigated factors.

§ In order to verify if the ***D5*** molecules were effectively grafted on the *P25* powder, two washing procedures were tested. In the first the *P25* powder remaining after the centrifugation in experiments 6 and 7 was contacted with 10.0 mL ethanol and left at rest overnight; then the solution was centrifuged (3000 rpm, 26 °C, 15 min) and the powder was again contacted with 10.0 mL ethanol for 10 minutes; then the solution was centrifuged, added to the previous one and analyzed by UV-Vis. The second method differed only in the contact time of the first ethanol aliquot that was 10 min. The number of molecules removed by the two treatments was similar and about of the same order of magnitude of the estimated standard deviation, indicating that the molecules of ***D5*** are tightly bonded to the surface of titania and not only physisorbed and/or stacked on the surface in weakly bound multilayers.